Trabajo Fin de Grado
Grado en Ingeniería Civil

Analysis of the utilization of blast furnace slag as recycled aggregates in self-compacting concrete

Autor: Adelardo Vahí Sánchez de Medina
Tutor: Héctor Cifuentes Bulté
Carlos Leiva Fernández

Dep. Mec. Medios Continuos y Tª de Estructuras
Escuela Técnica Superior de Ingeniería
Universidad de Sevilla

Sevilla, 2017

Trabajo Fin de Grado
Grado en Ingeniería Civil

Analysis of the utilization of blast furnace slag as recycled aggregates in self-compacting concrete

Autor:
Adelardo Vahí Sánchez de Medina

Tutor:
Héctor Cifuentes Bulté
Profesor contratado doctor
Carlos Leiva Fernández
Profesor titular de Universidad
(Dpto de Ing. Química y Ambiental)

Dep. de Mecánica de Medios Continuos y Teoría de Estructuras
Escuela Técnica Superior de Ingeniería
Universidad de Sevilla
Sevilla, 2017

Abstract

In this article, a study for investigating the effects of replacing the aggregate of self-compacting concrete by blast furnace slag has been carried out. Different mixes have been made by substituting the fine and coarse aggregates. The fracture energy, the tensile strength and the compressive strength have been tested. The remaining properties of self-compacting, or the absence of them, have been observed.

This research can find goals such as decreasing the price of aggregates, reducing the industrial waste and attenuating the rate of consumption of natural resources.

The results show that the self-compacting property is gradually lost as the slag content is increased, so – when the ratio of replacement is low – the concrete keeps the self-consolidating properties. However, these losses affect to the mechanical properties.

1. Introduction

Blast furnace slag (BFS) is a nonmetallic industrial by-product, formed in blast furnaces with the melting of the iron ore, producing molten pig iron [1]. More than 500 million tons of blast furnace slag (BFS) are produced every year worldwide [2]. The blast furnace slag can be granulated slag (GBFS) or air-cooled slag (ACBFS). Granulated slag is cooled rapidly by using water, resulting in a vitreous slag, while air-cooled slag is slowly cooled by ambient air. The air-cooled slag solidificates and crystallizes, creating a rock-like slag [3].

The main use of blast furnace slag is cement production [4], which can be done by using granulated slag, but BFS can be used also as any other additive to concrete or as part of alkali activated materials [5] in the form of GBFS or ACBFS. Today, in the European cement regulations, there are 14 types of cement containing blast furnace slag [4].

In Spain, the 70% of slag produced in 2014 is recycled. However, the remaining 30% wasted - that represent half million of a tone – is deposited in landfills due to unknowledge about the recycling opportunities of this material [6]. Blast furnace slag can be used also in road construction [4], which is it main use in the USA. In there, in 2012, 68.6% of the ACBFS was used as road base, road surface layers and asphalt concrete, whereas only 13.1% of the ACBFS was used as aggregate replacement for concrete in the USA [7]. However, the demand for concrete has increased rapidly due to the development of industrialization and urbanization in the last decades. It is estimated that the world demands over 10 billion tons per annum of construction aggregates [8].

The use of blast furnace slag in the production of concrete can have economical motivations – acquiring blast furnace slag as a waste industrially generated is cheaper than obtaining natural aggregates from a quarry. Moreover, the reuse of blast furnace slag has implications in the enviromental preservation and promotes a sustainable development. In this way, is

important to investigate the use of slag in the production of concrete, either as an aggregate or as a binder [4].

The convenience of slag usage as aggregate in concrete will depend on the properties that have to be achieved, in fresh and hardened states. In this way, according with some authors [9], the concrete produced with blast furnace slag has more workability when fresh, facilitating the vibration and making a better compaction with less entrapped air. When investigating hardened properties, some researchs assure that a 50% replacement of cement with blast furnace slag can improve the mechanical properties and durability of concrete [10]. On the opposite, blast furnace slag replacing cement provokes lower strength during the early days due to a low initial rate of hydration [4]. This handicap can be fixed by the usage of chemical activators, by increasing its specific surface or by raising its temperature [11]. Consequently, depending on the application of the concrete, as well as on climate conditions, the rate of cement replacement by blast furnace slag will be different.

However, the depletion of the natural aggregates as well as the consumption of large amounts of energy on the production, transportation, and use of raw materials, should be considered when producing concrete [12]. With this consideration, the use of ACBFS as aggregate in concrete, must be taken into account.

According to [1], “during the past two decades, a series of studies have been undertaken to understand the behavior of concrete containing ACBFS aggregates [13–15]. These studies have shown that ACBFS aggregate concrete (SAC) has a great potential to be a feasible alternative to natural aggregate concrete (NAC) in the construction industry”.

The goal of this research is to investigate the effects of adding air-cooled blast furnace slag (from now on, recycled aggregate) in substitution of the natural aggregate on the properties of the self consolidating concrete. Some concretes samples have been made in order to test their compressive and tensile strength, to study how the fracture proccess happens and to

see how the bilineal tension softening diagram changes as the slag content increases. It is used both coarse and fine aggregate, and the effect of each one of them is studied separated and mixed.

2. Materials and methods

2.1 Materials

For the production of the different compositions studied in this work, several components have been used. The cement used was CEM-II/B-L 32,5N, fabricated according with EN 197-1[16]. The superplasticizer used was MasterGlenium 355C and MasterGlenium ACE 325. The fabrication of it has been done according with the European Standard EN 934-2 [17].

The natural fine aggregate (NFA) used was siliceous sand, while the natural coarse aggregate (NCA) used is was lime-filled. The recycled coarse aggregate (RCA) and the recycled fine aggregate (RFA) was all air-cooled blast furnace slag (ACBFS). The chemical composition of all of them is shown in Table 1. The measured density of NFA was 2.65g/cm^3, the density of NCA was 2.66 g/cm^3 and the density of ACBFS was 2.7 g/cm^3. The similarity between densities make this ACBFS to be an appropiate replacement of this aggregate.

Component	Cement	NFA	NCA	ACBFS
SiO_2	20.96	95.6	0.013	28.12
Al_2O_3	5.74	2.41	0.064	9.12
Fe_2O_3	2.46	0.08	0.016	0.42
MnO	0.10	-	-	-
MgO	1.50	0.02	-	6.06
CaO	60.89	0.09	55.743	51.14
Na_2O	0.36	0.28	-	0.19
K_2O	0.73	1.49	-	0.54
TiO_2	0.28	0.04	-	0.76
P_2O_5	0.17	-	-	-
SO_3	1.11	-	-	1.77
MnO_2	-	-	-	0.41
BaO	-	-	-	0.11
Loss on ignition	5.2	0.2	43.997	1.47

Table 1. Chemical compositions.

As can be seen in Table 1, ACBFS is essentially a limestone material with a high content of SiO_2 which make it composition to be an intermediate composition between the ones of NFA and NCA. Due to that, with low ratio replacements of slag, the global composition of concrete will not vary too much. However, it is important to remark that the mixes with NCA and fine ACBFS replacing the NFA will be mostly limestoned, while the composition with NFA and coarse ACBFS replacing NCA will be siliceous. A mix with only ACBFS will have a similar composition than a mix fabricated with both natural aggregates coarse and fine. The NCA has a large content of $CaCO_3$ which appears in Table 1 as CaO plus loss in ignition.

The measured granulometry of each aggregate used is shown in Figure 1.

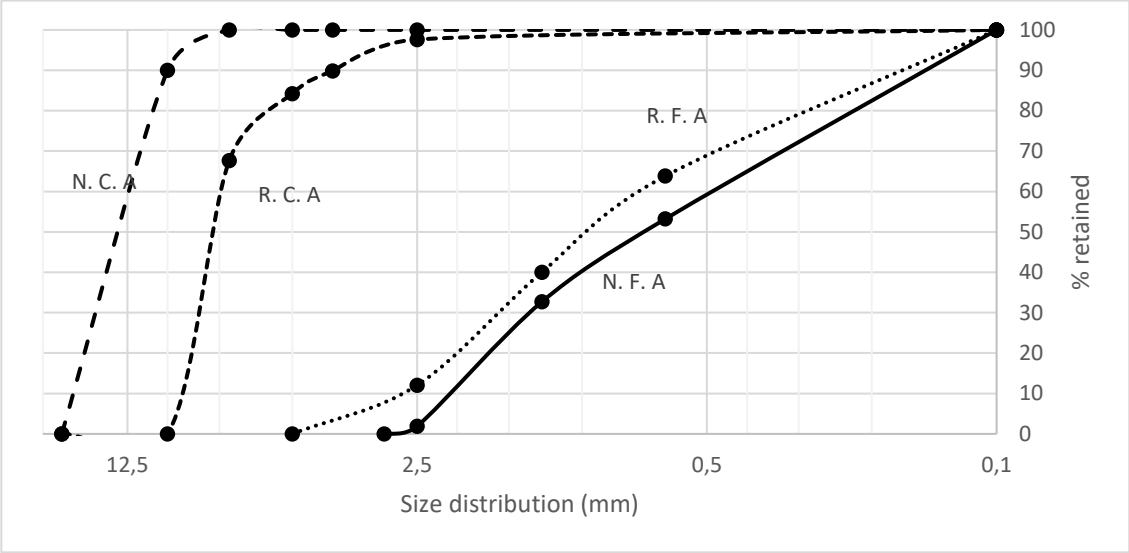

Figure 1. Granulometry of aggregates

As can be seen, the coarse slag is slightly smaller than the natural coarse aggregate. On the other hand, the fine slag is similar to the natural fine aggregate. This means that the range of particle size is narrower in the mixes where slag replaces natural aggregates.

As can be seen in Figure 2, the shape of coarse slag aggregate is different than the shape of natural coarse aggregate. Indeed, coarse slag grains show irregularities and cavities, while natural coarse grains have smoothen surface which lets a higher compaction.

Figure 2. Coarse slag aggregate (left). Coarse natural aggregate (right)

2.2 Compositions

Five different kinds of concrete were produced. The fabrication of the mixes has been done according with the specifications in the European standard EN 12390-2 [18]. The components used for each composition are shown in Table 2.

Composition / Material	I	II	III	IV	V
Cement (kg)	386				
Water (L)	194				
Fine natural agg (kg)	1040	520	1040	--	520
Fine recycled agg (kg)	--	520	--	1040	520
Coarse natural agg (kg)	693	693	346.5	--	346.5
Coarse recycled agg (kg)	--	--	346.5	693	346.5
Superplasticizer (L)	3.3				

Table 2. Composition of mixtures per m^3 of concrete

For each of the different compositions were produced 21 litres, which were casted into four specimens of 4.4 litres each with prismatic form. The concrete prisms were cured under water for 42 days, higher than 28 days, so it can be considered that the strengthen process was fully completed. The temperature of the water was 20ºC..

During the mixing proccess of each type of concrete, it was observed how the paste and aggregate flew properly in the compositions I, II and III, as it happens in self-consolidating concrete. However, mixture IV had lost self-consolidating properties (see Figure 3). Due to the fact that composition IV has the lowest range in size particle, it was a mixture that demanded more water [19-21]. Following this idea, a fifth sample was done based on composition IV but with a higher content of water. The composition of this sample is named IV.b.

Figure 3. Mixture I (left) and Mixture IV (right)

To the composition I was made the Flow Table Test for determine the self consolidating properties and the consistency of fresh concrete, this test is define in the European Standard EN 12350-5 [22]. The time until reaching the spread diameter was less than a minute and the diameters of the final shape were 70 centimeters (the longest one) and 62 centimeters (the shortest one). Both of them are perpendicular to each other. Also, it could be checked that there was no seggregation, as can be seen in Figure 4. This displacement of the aggregates happened in all the directions, and they moved as much as the cement paste, as can be seen in Figure 4.

Figure 4. Flow Table Test

The specimens have a prismatic form. These prisms were 44 centimeters long, and with a

squared cross section of 10 centimeters each side.

Considering that the self-consolidating properties are lost when recycled aggregate is added in high proportions, it was assumed that mix V was not going to be self-consolidating also, so composition V had an extra-consolidation done. This extra-consolidation was executed with a vibrating table for 1 minute.

3. Methods

3.1 Density test

The first test done to each mix was to obtain its density. The density was calculated as mass per volume unit. Both units – mass and volume – were measured in hardened samples. For each composition, all samples were tested and the average data was calculated.

3.2 Compression test

Compressive strength is the most usually measured mechanical property of a concrete. Considering that concrete is a material with a good behaviour under compressive loads, the quality of a concrete can be measured by the compressive strength. Moreover, generally, a concrete with a higher compressive strength will have better mechanical properties and more durability.

The compression test is defined by the European Standard EN 12390-3 [23]. Cubic specimens with faces of 10 cm long in each side suffer a increasing compressive load applied in the top face until the fracture of the material happens. Four specimens were tested for each mix. The compression was applied on a top face and a bottom face, letting the lateral faces free for displacements in all the directions. The velocity of the test is controlled by the displacement of the top face, which gets strained at a pace of 0.5mm/min. When compressive strength (f_c) is reached, the cube collapses and the test finishes. The maximum load applied to the cube before reaching the collapse, is the value of f_c for this sample.

The displacement of the top face and the load applied to the specimen were recorded each 0.2 seconds.

3.3 Barcelona test

Barcelona test, also known as double-punch test, let to know the tensile strength of concrete

(f_t). This test is defined according to the specifications in the Spanish Standard UNE-83515 [24], which assign this test for fibre-reinforced concrete. However, according with previous authors [25], this test is also valid for mass concrete.

Cylindrical steel punches with a height of 20 mm and a diameter of 25 mm were placed at the centre of the top and the bottom surfaces of the specimen. The specimens used were cubic with faces of 10 cm long in each side. Four different samples for each kind of concrete have been tested.

The displacement of the metallic cylinder over the top face and the load applied to the concrete specimen were recorded each 0.2 seconds.

During the test, the cylinders suffer compression against the surfaces where they were colocated, until they penetrate on the concrete specimens. This penetration provokes a tension state inside the concrete, until the specimen gets broken. In this point, the maximum tensile stress (f_t) that the concrete can support, is reached.

Once the maximum load applied for breaking the specimen is known, the f_t can be measured by the formula of Chen and Yuan [26].

3.4 Three-point bending test

This test was done in order to measure the fracture energy according to the work-of-fracture method of RILEM. The fracture energy of concrete is an important parameter in the analysis of the mechanical behaviour of concrete structures [27].

The test was done directly on the initial prism specimens, with a length of 44 cm and squared bases of 10 cm long in each side. Before doing this test, a notch is done to the concrete. This notch goes parallel to the bases, with 5 centimeters of depth, and cuts completely a lateral face of the prism. The notch is done in the center of the prism, separated the same length (22 cm) to each base. The lateral length of each prism is 10 centimeters, so the ratio between

depth of the notch by total depth of the specimens was 0.5. In the middle cross section with the notch, the remainig area uncutted has a height of 5 cm and is 10 cm wide. This brings to a ligament area of 50 cm^2.

The notch is collocated looking downwards, so the face cut by it will be called the bottom face from now on, and in the opposite– the top face – will be where the load is applied. Since the modifications proposed by Guinea et al. [28-30] has been followed, the bending test is done compensating the self weight – some rubber bands were holding the prism for this.

The load is applied on the top face of it, in the center of that face, exactly over the notch, with a cylinder parallel to the bases of the prism. The load applied provokes displacements and strains, which are measured along with the value of the load. There is a record of data for each 0.25 seconds. In that way, there are four measurings taken each second for each of the four following magnitudes: the load applied to the top face, displacement of that face, strain of the bottom face according with a reference taken on the top face and the aperture of the notch in the bottom face.

There are two different stages in the test: firstly, the load applied is increased by making constant the increment of the displacement of the top face, which increases 0.2 mm each minute, until the load reaches a value of 0.2 kN. After this point, there is a second stage where the evolution of the test is controlled by the speed of opening of the bottom part of the notch, until the aperture of the notch has increased in 1mm since the beginning of the test. In this moment, the test finishes. When the aperture of the notch reaches 1 milimeter, there is a crack that can be seen going from the front of the notch to the top face. When the rubber bands are removed, the prism breaks following the route marked by the crack.

All prisms have been tested, so the final results for each material can be taken by an average of more than one sample (four samples as much), making it possible to discard the results of any test done wrongly.

3.5 Bilinear softening curve

With the results of the bending test, some parameters can be obtained with an iteration proccess. By using the real softening curve (which correlates Load and Notch widening), the Elastic modulus and the f_t can be calculated. Also, three more data (a_1, a_2 and b_2) which define the slopes of two straight lines (a_1, a_2) and the zero crossing of one of this lines with vertical axis in the diagram (b_2). With this five data, it can be represented the bilinear approximation of the theorical correlation mentioned before – Load-Notch widening – as can be seen in Figure 5. The final result is a three-line graph that represent some of the main properties of each concrete in a very simple way, just with linear correlations.

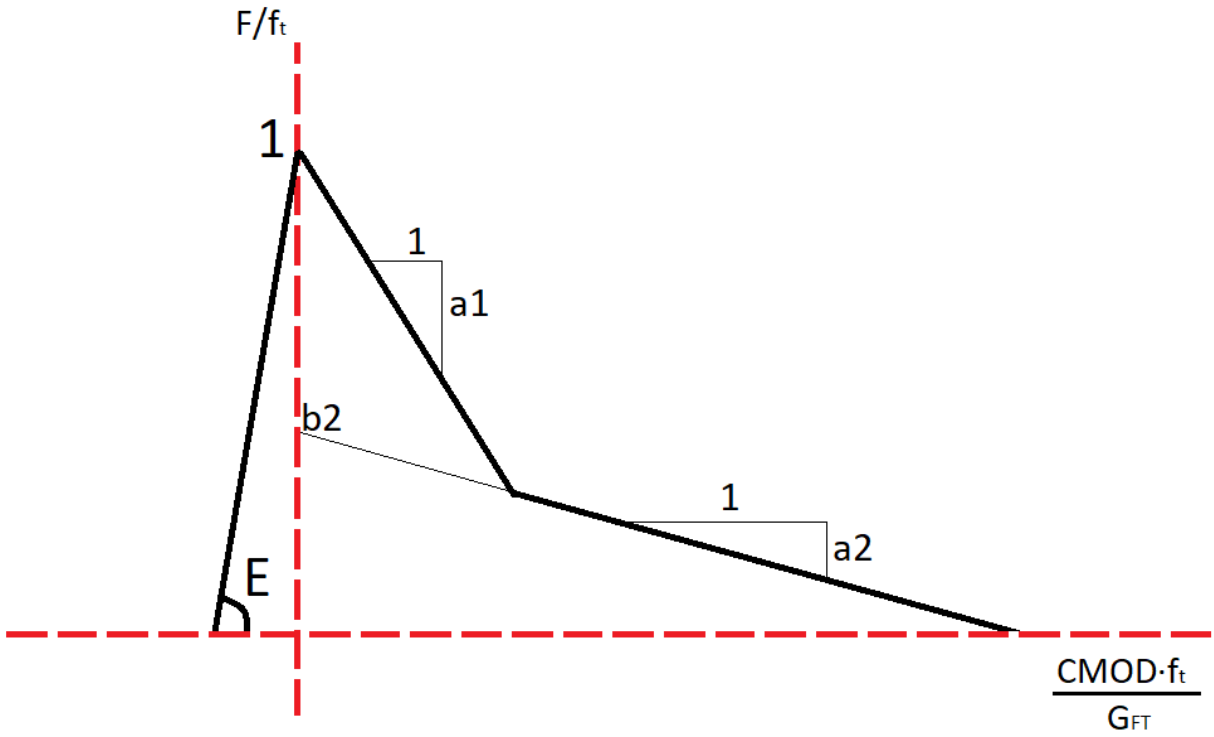

Figure 5. Load (F) – Notch opening (d) bilineal correlation

4. Results

4.1 Density test

The results obtained are shown in the Table 3.

Mix	I	II	III	IV	IV.b	V
Density (kg/m^3)	2.28	2.21	2.17	1.97	2.15	2.31
% standard deviation	0.98%	1.88%	2.64%	1.22%	--	2.63%

Table 3. Density of mixtures

As can be seen in Table 3, the adition of slag leads to a decrease in density. Cement and water content have not changed between different mixtures and density of different aggregates is quite similar, so density depends mostly in porosity. Mix II, where replacement of aggregate is equal to 50% of fine aggregate, shows a decrease of 3% in density, while the replacement of 50% in the coarse aggregate shows a decrease of 5% in density, when compared with composition I. In fact, mix II has a slightly higher granulometry that explains the higher porosity which causes this decrease on density, meanwhile mix III is made with coarse slag aggregate, which – as could be seen in Figure 2 – had irregularities and cavities in the surface of the grains, causing the lower density on the mixture when compared with mix I. Moreover, a wider particle size distribution causes a higher packing density and decreases water demand, while a narrower particle size distribution gives higher hydration rates for equal specific surface area [19-21]. Mix III has a narrower particle size distribution, however the proportional amount of water was not changed between different mixes, which provokes a decrease in density.

However, the density of composition IV, which had a full replacement of aggregate by slag, is 13.5% lower than density of composition I, and the absolute data was 1.97 kg/m^3, which is extremely low compared with an average concrete density. This matches with the

excessive porosity that it showed in Figure 3. The variation of density between mixes I and IV are an emphasis of the variation of density between mixes I and II or mixes I and III. All the reasons why density was lower in mix II and in mix III have a combinated effect in mix IV.

This excess of porosity was tried to be corrected by adding more water to the mix, which corrected the density by increasing it a 9%, which means having a density 6% lower than mixture I.

With this information, we can sentence that a full replacement of aggregate by blast furnace slag, affects to density.

However, mix V did not show any porosity. Therefore, mixes I and V have very similar densities. The difference of density in mix V is only around 1.5% in relation to mix I, which suggests that the self consolidation of mix I worked as good as the vibration. Aggregates in mix V are smaller than aggregates in mix I, which explains the slightly less porosity that it have.

4.2 Compressive strength

The result obtained on this test consist on the nominal stress produced by the maximum load applied to the specimen, when it is supposed a uniform distribution of the stresses.

The results are shown in Table 4.

Material	I	II	III	IV	IV.b	V
f_c (MPa)	41.16	26.48	26.83	11.82	27.89	56.69
% standard deviation	4.5%	7.9%	20.2%	12%	--	4.2%

Table 4. Results of Compression Test

It can be seen that the concrete made with both coarse and fine slag replacing half of the aggregate has better compressive properties when vibrated than the self-compacting

concrete made only with natural aggregate – this improvement is over the 35%. Therefore, it can be assured that fewer costs in the material can create a significantly better material, but assuming the renounce of a self-consolidating concrete, which can be an interesting fact considering the increasingly concern of the waste of materials.

Without vibration, the slag provokes a descent on the compressive strength when compared with the mix made only with natural aggregate. If the replacement of aggregate is not accompanied with an extra vibration, the f_c of concrete is reduced by 35% when the amount of replaced aggregate is 50% of one of the two kinds of aggregates. There is no evidence of difference between replacing coarse aggregate or fine aggregate. This descent is situated around the 70% when all the aggregate is replaced. The excess of porosity reflected in a lower density is a cause for having less compressive strength in a concrete [31].

The sample of composition IV.b, which was made by adding an extra quantity of water to the mix, was tested also for checking its compressive strength, resulting in a sample with a value for the f_c of 27.89 MPa, more than twice the value of the average of sample IV. This fact can lead us to considerate that the replacement of aggregate by slag should be done along with a higher use of water.

4.3 Tensile strength

When Barcelona test is applied to concrete without fibres, the f_t can be obtained by applying the formula proposed by Chen and Yuan [26]. This formula uses geometrical parameters of the test and the maximum load applied before the concrete cube breaks.

The average maximum load and f_t obtained with this test for each kind of concrete Is shown in the Table 5.

Material	I	II	III	IV	IV.b	V
Maximum load (N)	81175	71250	69550	20016	32500	80325

f_t [26] (MPa)	3.32	2.91	2.84	0.67	1.32	3.28
% standard deviation	4.8%	3.0%	12%	13.9%	--	15.3%

Table 5. Results of Barcelona Test

As a conclussion, we can say that the addition of slag creates concretes with lower tensile strength. This reduction is located between 12% and 14% when only 50% of one of the kind of natural aggregates is replaced (mixtures II and III). When the replacement of aggregate is total and the amount of water added does not change, the f_t falls down an 80%. The external appearance of this mix, suggested that it could not be used for structural usage, and the low data of f_t reached is a hard evidence of this.

However, this composition improves its properties notably by adding more water to the mix. When the replacement of aggregates by slag is superior than it in mixes II and III, but the concrete is vibrated, the f_t remains in similar values than that obtained with just natural aggregates.

4.4 Fracture energy

The results from three-point bending tests are shown in curves correlating the load applied with the vertical displacement produced in the bottom face (face with the notch) of the prism. The area covered by this graph is the so-called work-of-fracture. In Figure 6, the average Load-displacement curve for each material is shown.

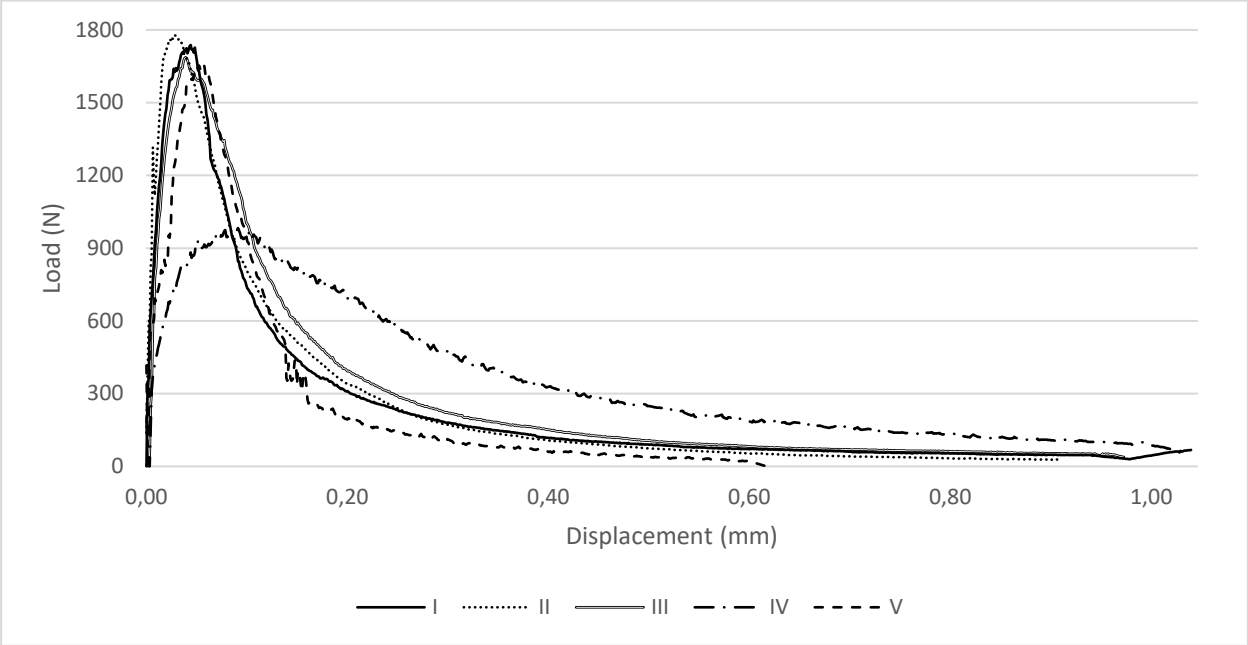

Figure 6. Load - Vertical displacement for different mixtures

The average fracture energy per area for each material (G_F) and the maximum load reached for each concrete is shown in Table 6. As said before, the uncutted area in the cross section with the notched has 50 cm^2.

Material	I	II	III	IV	V
Maximum load (N)	1847	1861	1728	966	1831
G_F (N/m)	51.28	51.28	56.7	75.29	46.47
% standard deviation of G_F	19.4%	10.3%	16.5%	10.2%	33.8%

Table 6. Results of Bending Test

According with previous authors [28-30], the specific fracture energy of each mix can be calculated by the method RILEM with some modifications. The RILEM method needs various ratios of depth of the notch and does not consider the compensation of self weight. The fracture energy obtained is not a real constant on the material because it depends on the size of the sample. With this modifications, the fracture energy is calculated as the area

covered by the curves shown in Figure 6 plus an extra area that can not be measured when the self-weight is compensated, which correspond to the asymptotic area. This extra area can be estimated by adjusting the tail of the load-displacement curve [32]. Taking a point (δ_u) in the right-side of the curve – where the test was stopped – and considering the load in this point (P'(δ_u)) to be fictionally 0, the non-measured work of fracture that can not be measured directly is considered to be $\frac{2 \cdot A}{\delta u}$, where A is the value that gives a best approximation of the shape of the curve at the left of δ_u, when this shape is calculated as an hyperbole $P' = A \cdot (\frac{1}{\delta^2} - \frac{1}{\delta_U^2})$, where δ is the displacement and P' is the load depending on displacement and taking as a virtual reference P'(δ_u)=0.

As shown in Table 6, the G_F of mixtures I and II is equal, meanwhile the substitution of coarse aggregate leads to a increase in the G_F, being this increasement of 10.5%. With the highest usage of slag (mixture IV), when it replaces all the natural aggregate, the G_F reaches its top, increasing a 47% more than concrete with natural aggregate.

The average G_F obtained for mixture V is the lowest of all mixtures, which maybe shows that this concrete has less ductility. The G_F is a 9% lower than in the reference concrete, however the deviation calculated of the different samples which have been tested is too high (33.8%), which shows hesitation over this data.

One aspect to take in account is the fact that mixtures with lower G_F has a higher maximum load. All curves of the different samples vary from sharped to wider. As can be seen in Figure 6, the highest peak loads are obtained with a lower vertical displacement, and as the peaks of the curves gets lower, they tend to be more to the right. The extreme situation is mix IV, which despite having a maximum load of around 50% of the maximum loads of the other mixes, it covers a wider area, with the pre-peak curve less vertical and the decrease of post-peak curve softer.

4.5 Bilinear softening curve

The bilinear approximation of the real softening curve (Bilinear softening curve) presents the average results for each mixture shown in Table 7.

Material	I	II	III	V
f_t	3.09	3.36	2.81	3.37
a_1	39.9	40.2	30.8	39.4
a_2	0.42	1.79	0.92	2.18
b_2	0.100	0.199	0.149	0.193
E	29181	25412	24651	25627

Table 7. Parameters for Bilinear softening curve.

The load-displacement curve obtained in bending test for mix IV is very different of the curve that should be obtained for an adequate concrete. The non-linearity of pre-peak part of the curve and the similarity between the two slopes in the post-peak zone made it impossible to find a bilinear softening curve with a low enough tolerance.

For all the other mixes, bilinear softening curve are shown in Figure 7. It can be observed that slag aggregate causes always a disminution on the value of the modulus of elasticity. This disminution varies between 12.9%, 15.5% and 12.2% for mixes II, III and V respectively.

The similarity between mixes II and V remains in the other parameters, making both curves very similar one to the other. The mix III, however, shows a shorter peak (lower f_t) and a more horizontal slope at the right of the peak, meaning that mix III is a weaker material in the elastic phase but more energy is needed for the propagation of the cracking [33]. Tensile failure in concrete can be caused by tensile failure of aggregates or by cracking in the surface between aggregate and cement paste [34]. Considering this, the size of aggregates in mix III was smaller than in mixes I, II and V, and this make shorter the route for propagation of cracking

between surfaces of aggregates. For this reason, the cracking in mix III grows following an irregular path and avoiding the aggregates, while in mixes I, II and V – with larger aggregates – this path would be much longer so the cracking is produced following a straighter route, cutting the aggregates (so it is necessary a higher f_t) but once they are cut, having an easier and shorter growth of fracture.

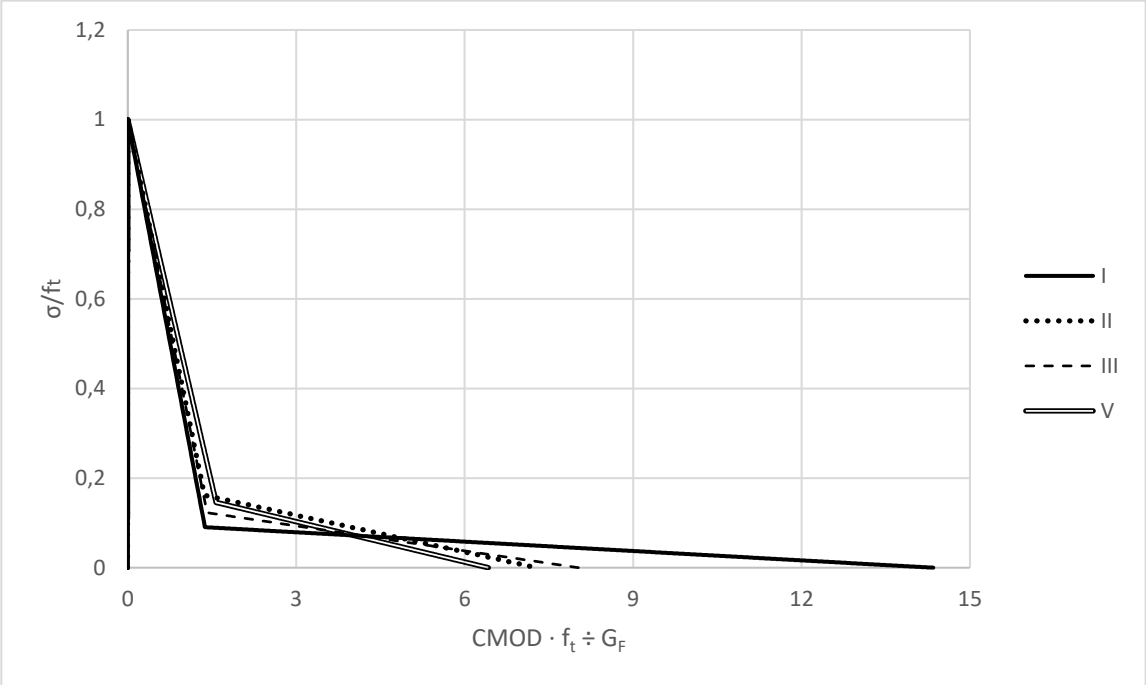

Figure 7. Bilinear tension softening diagram

According with some authors [36], the value of a_2 is a result of the aggregate interlock which is primarily governed by the maximum size and texture of the coarse aggregate used in the concrete mix. As mentioned before, the texture of the coarse slag is different, with more irregularities, than the texture of the coarse natural aggregate. Moreover, the mixes with slag have a higher slope in a_2, resulting in a concrete with lower ductility. However, this influence also appears in mix II, which does not have coarse slag but fine slag, suggesting that texture in fine slag can also has an effect on the value of a_2. The behaviour of parameter a_1 is governed by the micro-cracking [35],

which is a property related with the ratio water/cement. This ratio was mantained in mixes I, II, III and V, which explains the similarity of a_1 values.

The pre-peak phase depends on two of the properties of concrete: elastic modulus and tensile strength. As can be seen in Figure 8, mix I is the most rigid mix, but a replacement on fine aggregates can increase tensile strength, even if this mixes are less rigid. Coarse slag – with irregular shape, more porous and with smaller grains – creates a material with a lower tensile strength and less rigidity.

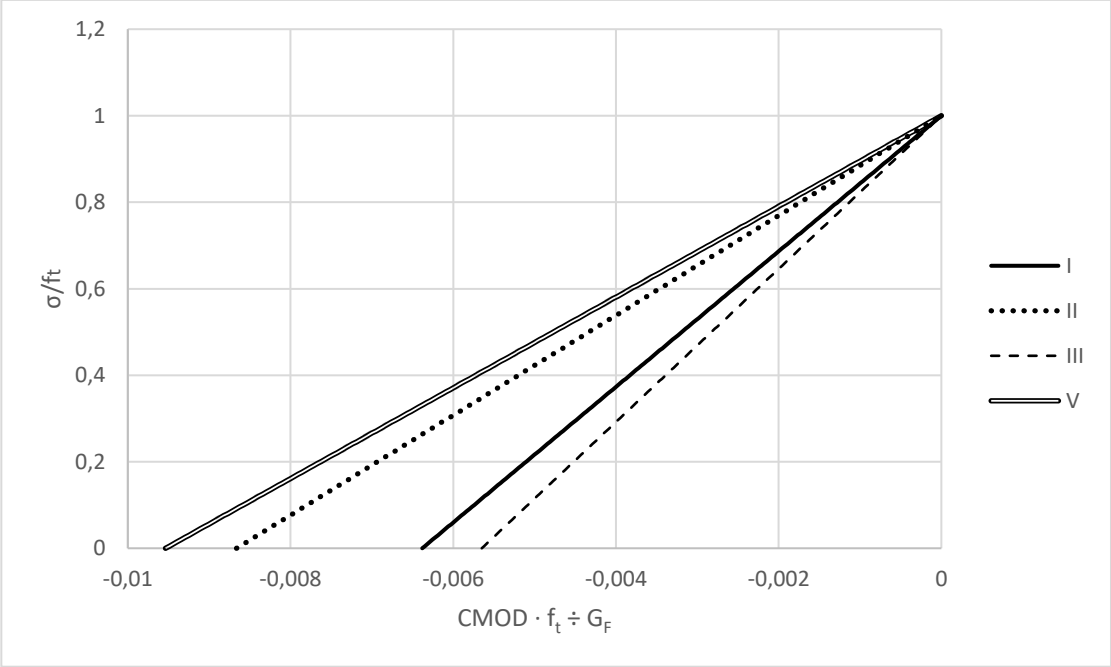

Figure 8 – Pre-peak phase. Bilinear tension softening curve

Ahead of the crack, there is a zone where material is being in tension and all the deterioration mechanisms to produce the cracking of concrete are produced. This zone is called Fracture Process Zone (FPZ) and it size is related with the ductility of the material – the larger this area is, the more ductility has the material. However, it is not simple to calculate the size of it. Associated with this magnitude, the characteristic length (l_{ch}) of a material is considered to be proportional to the size of FPZ [32]. A longer l_{ch} means a larger FPZ, and l_{ch} is calculated with the formula $l_{ch} = \frac{E_c * G_{FT}}{f_{ct}^2}$ [35]. l_{ch} values are shown in Table 8.

Material	I	II	III	V
l_{ch}	165.3	120.2	182.8	147

Table 8. Characteristic length (mm)

As it was mentioned before, mixtures with a higher f_t tend to be mixtures with a lower G_F. Considering that l_{ch} is proportional to G_F and inverse to f_t, mixture III – which had previously the highest value of G_F between the mixtures with bilinear correlation calculated – is now the mixture with a higher value of l_{ch}, which means the more ductil of them. l_{ch} value is directly related with maximum coarse aggregate size [35], but for mixes I and II, the maximum coarse aggregate is the same, so the depletion of value produced, of around 27%, suggests that fine slag produces concretes with lower ductility than natural fine aggregate. The l_{ch} of mixture V is between the values for mixture II and mixture III, probably influentiated by the reasons that make l_{ch} of II gets lower and also the reasons that make l_{ch} of mixture III higher. Moreover, the lower l_{ch} correspond to the sharper curves mentioned before, meanwhile the longest l_{ch} are related with the widest curves.

With the parameters obtained for Bilineal Softening Curve of mix III, the Load-CMOD curve of these mix would be the dotted line represented on Figure 9. The real curve obtained with the data test is represented also as comparison.

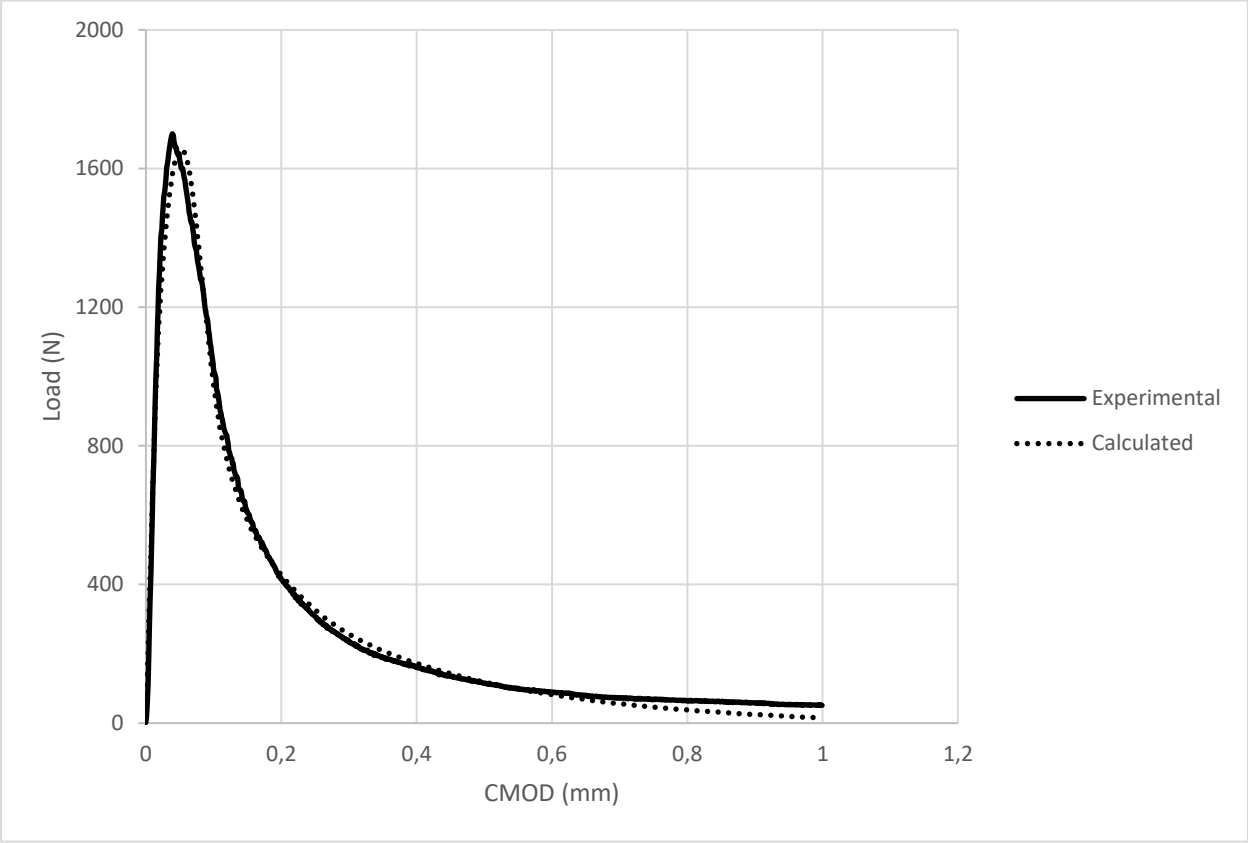

Figure 9. Experimental curve and curve calculated with method of RILEM modificated for mix III

5. Conclusions

The results of this research show that blast furnace slag is not an appropiate material for replacing the totality of aggregate needed in the production of self-compacting concrete. However, it is an interesting partial substitute that in certain doses maintain the self-compactibility properties of the concrete. For non self-compacting concretes, the blast furnace slag conservate and even can improve the mechanical properties of concrete made with natural aggregates.

The substitution of aggregate can not be total if the slag concrete is not going to be vibrated. Even with partial substitutions, not close to a full replacement, the mechanical properties are substantially lost. If there is an option for vibrating the concrete or if the substitution is made in low amounts (less than 25% of total aggregate), the mechanical properties resultant are still high enough for structural purposes.

All this, along with the enviromental advantages that usage of blast furnace slag shows, make it a interesting material in the production of self-compacting concrete for low replacements.

6. Acknowledgements

The authors acknowledge the collaboration of Emilio Javier Gómez Álvarez during the lab work. We are also grateful for the donations made by Taljedi S.A., supplier of natural coarse aggregate used, and by EDERSA, which supplied the blast furnace slag used. This work was partially funded by the Ministerio de Economía y Competitividad of Spain through the project BIA 2016-75431-R.

7. References

[1] Ozbakkaloglu, T., Gu, L., Fallah Pour, A. Normal- and high-strength concretes incorporating air-cooled blast furnace slag coarse aggregates: Effect of slag size and content on the behavior. Adelaide, 2016

[2] S.S. Yearbook, W.S. Association, Worldsteel Committee on Economic Studies, Brussels, 2014

[3] Visited 27th November http://www.slg.jp/e/slag/kind.html

[4] Bansode, S., Netinger Grubesa I., Fucic, A., Barisic, I. Characteristics and Uses of Steel Slag in Building Construction, 2016

[5] C. Leiva, C. Arenas, H. Cifuentes, L.F.Vilches, J.D. Ríos, B. Peceño. Development of materials for passive fire protection composed mainly by blast furnace slags

[6] Visited 27th November https://unesid.org/acero-y-sociedad-medio-ambiente-escorias.php

[7] Oss, H.G.v., Slag, Iron and Steel. 2013 Minerals Yearbook, US Geological Survey, Washington, DC, 2015. 26.

[8] Pacheco-Torgal, F., Ding, Y., Jalali, S. Properties and durability of concrete containing polymeric wastes (tyre rubber and polyethylene terephthalate bottles): an overview, Constr. Build. Mater. 30, 2012, 714–724.

[9] Hooton, R.D. Canadian use of ground granulated blast-furnace slag as a supplementary cementing material for enhanced performance of concrete, Can. J. Civil Eng. 27, 2000, 754–760.

[10] Berndt, M.L. Properties of sustainable concrete containing fly ash, slag, and recycled concrete aggregate, Const. Bldg. Mat. 23, 2009, 2606–2613.

[11] Valcuende, M., et al. Shrinkage of self-compacting concrete made with blast furnace slag as fine aggregate, Const. Bldg. Mat. 76, 2015, 1–9.

[12] Akçaözog˘lu, S., Atis, C.D. Effect of granulated blast furnace slag and fly ash addition on the strength properties of lightweight mortars containing waste PET aggregates, Constr. Build. Mater. 25 (10), 2011, 4052–4058.

[13] Valcuende, M., Benito, F., Parra, C., Miñano, I. Shrinkage of self-compacting concrete made with blast furnace slag as fine aggregate, Constr. Build. Mater. 76, 2015, 1–9.

[14] Ashby, J. Air cooled blast furnace slag as a concrete aggregate for engineering construction, in: National Symposium on the Use of Recycled Materials in Engineering Construction: 1996, Programme & Proceedings: Institution of Engineers, Australia, 1996. 110.

[15] Jariyathitipong, P., Hosotani, K., Fujii, T., Ayano, T. Strength and durability of concrete with blast furnace slag, in: Third International Conference on Sustainable Construction Materials and Technologies, Kyoto, Japan, 2013.

[16] EN 197-1, Cement - Part 1: Composition, specifications and conformity criteria for common cements, CEN European Committee for Standardization, Brussels (2011)

[17] EN 934-2, Admixtures for concrete, mortar and grout - Part 2: Concrete admixtures - Definitions, requirements, conformity, marking and labelling, CEN European Committee for Standardization, Brussels (2010)

[18] EN 12390-2, Testing hardened concrete - Part 2: Making and curing specimens for strength tests, CEN European Committee for Standardization, Brussels (2009)

[19] Aiqin, W., Chengzhi, Z., Ningsheng, Z. The theoretic analysis of the influence of the particle size distribution of cement system on the property of cement, Cem Concr Res 29, 1999 1721–1726.

[20] Kuhlmann, K., Ellerbrock, H.G., Sprung, S. Particle size distribution and properties of cement, Part I: strength of portland cement, ZKG 6 1985, 136–145

[21] Visited 27th November https://ac.els-cdn.com/S0032591008003252/1-s2.0-S0032591008003252-main.pdf?_tid=cc7bafee-d3a2-11e7-8477-00000aab0f27&acdnat=1511808363_3bfbef7628781a49e4fadcd3436628f6

[22] EN 12350-5, Testing fresh concrete - Part 5: Flow table test Consultado el 28 de noviembre, CEN European Committee for Standardization, Brussels (2009)

[23] EN 12390-3, Testing hardened concrete - Part 3: Compressive strength of test specimens, CEN European Committee for Standardization, Brussels (2009)

[24] Asociación Española de Normalización y Certificación, Hormigones con fibras. Determinación de la resistencia a fisuración, tenacidad y resistencia residual a tracción. Método Barcelona, UNE 83515, Madrid, 2010.

[25] Guardia J. y Molins C. Caracterització del Comportament a Tracció del Formigó D´Alta Traballabilitat Reforçat amb Fibres D'Acer Mitjançant L'Assaig Barcelona. 2008-PI-01, Cátedra BMB Innovación en tecnología del hormigón. Publicacions del Dept. d'Enginyeria de la construcció, Barcelona, 2008, 290 pp.

[26] Chen W.F., Yuan R.L. Tensile strength of concrete: double punch test. J Struct Div 1980, 106(8):1673–93.

[27] Cifuentes, H., Alcalde, M., Medina, F. Measuring the Size-Independent Fracture Energy of Concrete. Strain, 49, 2013, 54-59.

[28] Elices M., Guinea G.V., and Planas J. Measurement of the fracture energy using three-point bend tests: Part 3 – influence of cutting the p-delta tail. Materials and Structures, 1992, 25(6):327-334

[29] Planas J., Guinea G.V., and Elices M. Measurement of the fracture energy using three-

point bend tests: Part 1 – influence of experimental procedures. Materials and Structures, 1992, 27(4):99-105

[30] Planas J., Elices M., and Guinea G.V. Measurement of the fracture energy using three-point bend tests: Part 2 – influence of bulk energy dissipation. Materials and Structures, 1992, 25(5):305-312

[31] Felekoglu, B., Turkel, S., Baradan, B. Building and Environment, 2007, 42, 1795-1802

[32] Cifuentes, H., Medina, F. Mecánica de la fractura aplicada al hormigón, Secretariado de Publicaciones, Universidad de Sevilla, 2013.

[33] Cifuentes, H., Leiva, C., Medina, F., Fernández-Pereira, C. Effects of fibres and rice husk ash on properties of heated HSC. Magazine of Concrete Research, 2012, 64, 5, 457-470

[34] Zhou. X.Q., Hao, H. Mesoscale modelling of concrete tensile failure mechanism at high strain rates. Computers and Structure, 2008, 86:2013-2026.

[35] Alyhya, W.S., Abo Dhaheer M.S., Al-Rubaye, M.M., Karihaloo, B.L. Influence of mix composition and strength on the fracture properties of self-compacting concrete, 2016.

[36] Abdalla, H. M., Karihaloo, B.L. A method for constructing the Bilinear tension softening diagram of concrete corresponding to its true fracture energy. Magazine of Concrete Research, 2004, 56, 597-604